RPE | Radiation Physics & Engineering
A Peer-Reviewed Journal
Published by K.N. Toosi University of Technology
http://rpe.kntu.ac.ir
Research Article

Radiation Physics and Engineering 2025; 6(2):23–34

Numerical and CFD analysis of inclination angle effects on natural circulation mini-loop performance

Sayed Abolhasan Nourashrafeddin, Mohsen Shayesteh*
Department of Physics, Faculty of Science, Imam Hossein University, Tehran, Iran

HIGHLIGHTS

- Natural circulation in a mini-loop and stability map of a closed loop is investigated.
- The influence of the angle of inclination of the loop on the stability map is studied.
- Effect of loop inclination angle on the mass flow rate and on the temperature difference across heater is studied.

ABSTRACT

This research simulated the natural circulation within a mini-loop using numerical calculations performed with a FORTRAN code and CFD simulations via Ansys Fluent. A stability map of the loop was derived, and the impact of the loops inclination angle on this stability map was examined. The findings indicate that at low power levels, particularly functional powers, the loops inclination angle does not significantly affect the stability map. The results of the numerical calculations were compared with Vijayans experimental corrections for this mini-loop, showing good agreement within its functional power range. Additionally, a comparison was made between the numerical calculations and the Ansys Fluent simulation results, which also demonstrated a good agreement, thereby confirming the accuracy of the calculations. Two significant thermo-hydraulic parametersthe mass flow rate and temperature difference at the two heater headswere calculated and compared for different loop inclinations. It was observed that increasing the inclination angle results in a decrease in the fluids mass flow rate and an increase in the temperature difference at the ends of the heat source. Notably, it was determined that achieving a specific temperature difference across the heat source does not necessarily require adjusting the power levels; simply changing the inclination angle is sufficient. Another important result of this research is that by making a series of straightforward assumptions, one-dimensional computations can be solved very precisely, thereby saving computation time.

KEYWORDS

Mini-loop
Natural circulation
Ansys fluent
Inclination angles
Fortran code
Thermo-hydraulic parameters
Numerical calculations

HISTORY

Received: 2 September 2024
Revised: 4 November 2024
Accepted: 8 November 2024
Published: Spring 2025

Nomenclature

A	cross section
b	constant number in friction factor equation
ω	dimensionless mass flow rate
g	gravity acceleration
H	height
K	thermal conductivity
L	length
C_p	specific heat capacity
Q	power
S	space coordinate
T	temperature
t	time
U	heat transfer coefficient
V	volume
W	flow rate
P	constant number in friction factor equation
q''	heat flux
D	Diameter
$\bar{f}$	friction factor
μ	viscosity
Δ	difference
ΔP	pressure loss
τ	Dimensionless time
α	Inclination angle

Subscripts

Ss	steady state
Hl	hot leg
cl	cold leg

*Corresponding author: Mshayesteh@ihu.ac.ir

https://doi.org/10.22034/rpe.2024.476581.1240

t	total
s	secondary side
m	modified
i	space summation in finite difference
n	time summation in finite difference

1 Introduction

The basis of the natural circulation loop is that without the need for mechanical pumps, heat is taken from the heat source and given to the heat sink. Considering that the density of the fluid decreases with increasing temperature and vice versa increases with decreasing temperature, so the heat sink is placed at a higher height than the heat source in order to establish a natural circulation flow due to the acceleration of gravity (Marchitto and Misale, 2018). In this way, the difference in density in the cold and hot areas creates a buoyancy force in the loop, which plays the role of fluid driving force (Bocanegra et al., 2022). Natural circulation plays a very important role in all applications that require passive safety systems and is the basis of many innovative technologies due to its inherent functional characteristics (a natural passive method) (Zweibaum, 2015). In particular, as an important example, new developments in nuclear applications (such as fifth-generation power plants) require in-depth investigation of passive safety systems used in research and power facilities (Borreani et al., 2017). As we know from past nuclear accidents, the safety of nuclear systems is strongly related to their cooling systems, not only during normal operation, but also for the entire time that nuclear fuel is present in the plant (Kim et al., 2016). Therefore, the use of passive systems is one of the most important issues in the new applications of nuclear power plants.

In the initial moments after the shutdown of a nuclear power plant, up to 7% of thermal energy is produced, meaning that there is a significant amount of thermal energy that must be removed by the cooling fluid even after the plant is shut down (Chen and Yang, 2022). The International Atomic Energy Agency has presented several studies on natural circulation applied in advanced water-cooled reactors (Ahmed et al., 2020). Natural circulation is associated with challenges such as low driving force, low mass flux and stability effects, which can be widely used if properly solved (IAEA, 2021). Flow instability is a potential threat in natural circulation systems that prevent their widespread use (Luo et al., 2024). Extensive research has been carried out on the sustainability of natural circulation systems. One study focused on the impact of loop diameter on system stability, revealing that in single-phase systems, stability decreases with an increase in diameter. Conversely, in two-phase systems, stability enhances as the circuit diameter grows (Vijayan et al., 2008). Another study investigated the impact of flow direction on the stability of the natural circulation system by analyzing the steady state for both clockwise and counterclockwise circulation in a rectangular loop, with the heat source and heat sink arranged horizontally and vertically within the loop (Vijayan et al., 2007). The stability of a rectangular loop was investigated by altering the height-to-width ratio, with findings indicating that the loop becomes increasingly unstable as the ratio approaches one (Chen, 1985). The stability behavior of the Genova natural circulation loop was studied using numerical methods, with comparisons made to experimental results in some cases (Moussavian et al., 2003). Similarly, numerical calculations for both steady and transient states of the Genova loop were performed using implicit, explicit, and Crank-Nicholson methods (Karami and Aghaie, 2017). Additionally, computational fluid dynamics (CFD) calculations were conducted using Ansys Fluent software, and the results were compared with existing data, showing good agreement (Nourashrafeddin et al., 2023a). Experimental investigations into the stability of a mini-loop with single-phase natural circulation were conducted, focusing on the effect of loop inclination. It was found that only a 75-degree inclination significantly impacts fluid temperature, while temperature changes for vertical loops and inclinations of 30 degrees are minimal, similar to what is observed in large-scale natural circulation loops (Misale et al., 2007; Garibaldi and Misale, 2008; Misale, 2014). In a different study, Nourashrafeddin and colleagues (Nourashrafeddin et al., 2023b) simulated the single-phase natural circulation mini-loop examined by Garibaldi and Misale (Garibaldi and Misale, 2008) using Ansys Fluent software and compared the results with experimental data. Their findings showed good agreement for a loop diameter of 5 mm, suggesting that the experimental measurements of the mini-loop diameter might have been inaccurate (Garibaldi and Misale, 2008). Continuing research has highlighted that the inclination angle of the loop significantly affects NCL (Natural Circulation Loop) performance. As the inclination angle increases, the total circulation flow rate decreases (Zhu et al., 2013). Numerical studies have demonstrated that the steady-state mass flow rate declines with increasing loop inclination at a given power input (Bejjam and Kiran Kumar, 2019). However, incorporating an orifice can stabilize the flow at lower inclinations, although this results in a reduced mass flow rate and a larger temperature difference across the cooler section (Adarsh et al., 2020). CFD simulations have also effectively analyzed the impact of inclination on NCL behavior, with models accurately predicting experimental results (Zhu et al., 2013; Adarsh et al., 2020). These studies underscore the importance of considering the inclination angle in NCL design and operation, as it significantly affects thermal-hydraulic characteristics and overall system performance.

In this article, the aim is to investigate the natural circulation in a mini-loop with two methods of numerical calculations and CFD with Ansys Fluent software and when the loop is inclined as much as the angle around the axis perpendicular to its plane (this inclination angle is shown schematically in Fig. 1; Inclination Angle is specified by α symbol in figures) the effect of this inclination angle on thermo-hydraulic parameters such as mass flow rate and temperature difference between the two ends of heat source analyzed and investigated. The results of this analysis can help us in examining larger and more complex

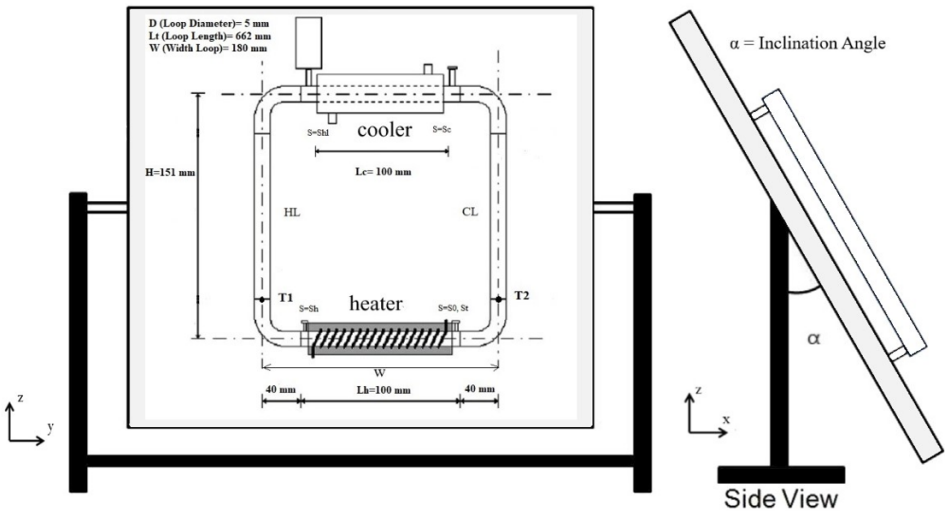

Figure 1: Schematic view of the natural circulation mini-loop.

systems in unstable environmental conditions. Considering that three-dimensional numerical solution calculations require more time than one-dimensional calculations, the results of these calculations and comparisons in this work can be used in solving many similar problems to save time using numerical solutions. Also, to achieve the desired temperature difference or mass flow, it is not necessary to change the power, but it can be achieved by changing the angle of inclination.

2 Material and Methods

2.1 System description and assumptions

In this study, a rectangular mini-loop with a circular cross-section (see Fig. 1) has been chosen as the thermo-hydraulic system for examining fluid natural circulation. The heat source is positioned at the bottom of the loop, delivering heat to the lower horizontal section with a constant heat flux. The cooling component is at the top of the loop, a heat exchanger maintained at a constant wall temperature (T_c), which is anticipated to be the lowest temperature point in the system. Both the heat flux and the cooling temperature (T_c) serve as variable parameters to assess system stability. The temperature difference across the heat source is represented by the difference between two points, T_1 and T_2, as illustrated in Fig. 1. These points are situated 40 mm from the lower section of the loop.

2.2 Numerical solution method

In this section, the numerical solution method employed by Karami and Aghaie (Karami and Aghaie, 2017) was utilized for calculating the mini-loop. The approach followed is similar to their method and a program written in FORTRAN language is used for numerical calculations. Here s represents the spatial coordinates along the loop and the origin is located at the beginning of the heat source. The calculations were based on the following assumptions:

- The diameter of the loop is the same in all sections,
- A single-phase and incompressible fluid (water at a pressure of 1 atm and a temperature range of 0-98 °C) is considered.
- The equations are solved in one dimension,
- The value of ρ is a constant value in all equations of conservation of mass, momentum and energy, except for the buoyant force, which is $\rho = \rho(T)$,
- Axial conduction heat transfer and viscosity change are not taken into account.

By simplifying the equations governing the fluid, we will have the following equations:
Energy equations:

$$\rho C_p\left(\frac{\partial T}{\partial t} + \frac{W}{\rho A}\frac{\partial T}{\partial s}\right) = \frac{4q}{D} \qquad \text{(for heater)} \tag{1}$$

$$\rho C_p\left(\frac{\partial T}{\partial t} + \frac{W}{\rho A}\frac{\partial T}{\partial s}\right) = -\frac{4h(T - T_s)}{D} \qquad \text{(for cooler)} \tag{2}$$

$$\rho C_p\left(\frac{\partial T}{\partial t} + \frac{W}{\rho A}\frac{\partial T}{\partial s}\right) = 0 \qquad \text{(for all sections except heater and cooler)} \tag{3}$$

Momentum equation:

$$\left(\frac{L}{A}\right)\frac{\mathrm{d}W}{\mathrm{d}t} + g\cos\alpha \oint \rho_0\Big[1 + \beta(T - T_0)\Big]\mathrm{d}z + \bar{f}\left(\frac{L_t}{DA^2}\right)\frac{W^2}{2\rho_0} = 0 \tag{4}$$

Mass equation:

$$\frac{\partial W}{\partial s} = 0 \tag{5}$$

In this study, we assume a constant density for the fluid due to the steady-state conditions of the system being analyzed. This simplification is justified because, in a well-insulated loop operating under stable conditions, changes in temperature and pressure do not significantly affect the density over the timescale of the analysis. The

mass flow rate of the flow along the loop is uniform at all times according to the assumptions that were considered. By applying the following dimensionless parameters according to the steady state conditions, the general equations stated above can be made dimensionless:

$$S=\frac{s}{H},\quad \omega=\frac{W}{W_{ss}},\quad Z=\frac{z}{H}$$
$$\tau=(\frac{W_{ss}}{V_t\rho_0})t,\qquad \theta=\frac{(T-T_{sec})}{(\Delta Th)ss} \tag{6}$$

Energy equations:

$$\frac{\partial\theta}{\partial\tau}+\frac{L_t}{H}\omega\frac{\partial\theta}{\partial S}=\frac{L_t}{L_h}\qquad \text{(for heater)} \tag{7}$$

$$\frac{\partial\theta}{\partial\tau}+\frac{L_t}{H}\omega\frac{\partial\theta}{\partial S}=-St_m\theta\qquad \text{(for cooler)} \tag{8}$$

$$\frac{\partial\theta}{\partial\tau}+\frac{L_t}{H}\omega\frac{\partial\theta}{\partial S}=0 \tag{9}$$
(for all sections except heater and cooler)

Momentum equation:

$$\frac{\mathrm{d}\omega}{\mathrm{d}\tau}-\frac{Gr_m}{Re_{ss}^3}\oint\theta\mathrm{d}z+\frac{P}{Re_{ss}^b}\Big(\frac{L_t}{2D}\Big)\omega^{2-b}=0 \tag{10}$$

Mass equation:

$$\frac{\partial\omega}{\partial S}=0 \tag{11}$$

where:

$$Re=\frac{WD}{\mu A},\quad Pr=\frac{\mu C_p}{k},\quad Nu=\frac{hL_t}{k}$$
$$St=\frac{hA}{C_pW},\quad St_m=\frac{4Nu}{Re_{ss}.Pr},$$
$$Gr_m=\frac{(g\cos\alpha)\beta D^3\rho_0^2Q_hH}{A\mu^3C_p}$$

It is assumed that the friction coefficient in the momentum equation is equal to $\bar{f}=\frac{p}{Re^b}$, which for the laminar flow $p=64$ and $b=1$ also for the turbulent flow Blasius corrections $p=0316$ and $b=025$ is considered.

2.2.1 Steady state solution

The steady state temperature distribution through the loop can be obtained using Eqs. (7), (8) and (9). The solutions are:

$$\big[\theta_h(S)\big]_{ss}=(\theta_{cl})_{ss}+\frac{H}{L_h}S\qquad \text{(for heater)}$$
$$\big[\theta_{co}(S)\big]_{ss}=(\theta_{hl})_{ss}\exp(St_mH\frac{S_{hl}-S}{L_t})\quad \text{(for cooler)}$$
$$Re_{ss}=\Big[\frac{2}{p}(\frac{D}{L_t})Gr_m\Big]^{\frac{1}{3-b}} \tag{12}$$

A schematic diagram of the mini-loop and the dimensions considered are given in Fig. 1. The output temperatures of the heat source and heat sink are equal to the temperature of the hot leg and the cold leg, respectively. With this equality, $(\theta_{hl})_{ss}$ and $(\theta_{cl})_{ss}$ can be obtained in the steady state conditions from Eq. (12):

$$\big[\theta_h(S=SH)\big]_{ss}=\big(\theta_{hl}\big)_{ss}$$
$$\big[\theta_{co}(S=Sc)\big]_{ss}=\big(\theta_{cl}\big)_{ss} \tag{13}$$

After many simplifications, the results can be expressed as follows:

$$\big(\theta_{hl}\big)_{ss}=\Big[1-\exp(-St_m\frac{L_c}{L_t})\Big]^{-1}$$
$$\big(\theta_{cl}\big)_{ss}=\Big[\exp(St_m\frac{L_c}{L_t})-1\Big]^{-1} \tag{14}$$

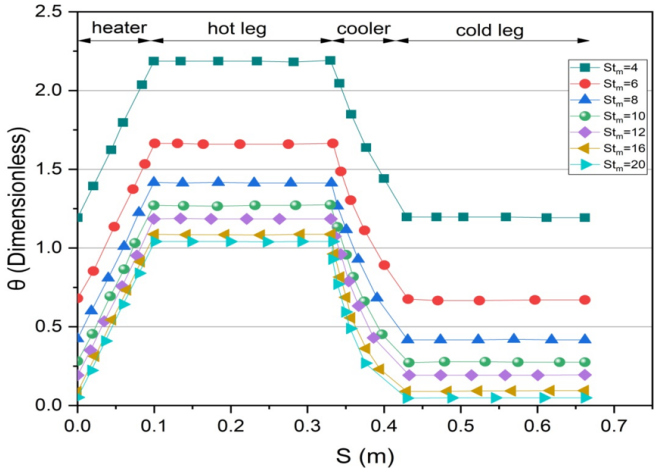

Figure 2: Temperature distribution along different sections of the rectangular mini-loop for different values of modified Stanton number.

Figure 2, obtained from numerical simulations using a program written in the FORTRAN language, shows the temperature distribution along a rectangular mini-loop for different modified Stanton numbers (St). The graph shows the dimensionless temperature (θ) across different sections: heater, hot leg, cooler, and cold leg. As St increases, the mass flow rate changes and, as a result, the temperatures decrease, especially in the hot and cooling leg sections. In the heater section, higher St values correspond to lower peak temperatures, indicating more effective heat dissipation. The hot leg exhibits constant temperatures, and higher values of St indicate decreased θ, indicating better cooling. In the cooling section, a significant temperature drop is observed at higher St values, which indicates effective heat removal. The cold leg stabilizes at lower temperatures, indicating more effective cooling at higher St values. These results show how increasing the Stanton number affects the heat transfer in the loop and leads to lower operating temperatures, which is important for optimizing thermal management. It should be noted that in these calculations, the system geometry and inclination angle are kept constant and only the modified Stanton number is changed to evaluate its effect on heat transfer. These results were obtained in steady state conditions and show that temperature changes are primarily due to changes in mass flow rate with increasing St values.

The total pressure drops along the loop can be given as Eq. (15):

$$\Delta p_{tot} = \bar{f}(\frac{L_t}{DA^2})\frac{W^2}{2\rho_0} \tag{15}$$

Using Eq. (12) and dimensionless parameters given in Eqs. (6) and (2.2), Eq. (15) can be written as follows:

$$\Delta p_{tot} = \frac{pL_t\mu^2}{2\rho_0 D^3}\left[\frac{2}{P}\left(\frac{D}{L_t}\right)Gr_m\right]^{(\frac{2-b}{3-b})}\omega^{2-b} \tag{16}$$

Assuming $\omega = \omega_{ss} = 1$ in Eq. (16), the steady-state pressure drop in the mini-loop can be determined. However, under transient conditions, the pressure drop along the loop is influenced by ω^{2-b}.

$$\begin{aligned} Re_{ss} &= 0.1768(\frac{Gr_m D}{L_t})^{0.5} \quad \text{(for laminar flow)} \\ Re_{ss} &= 1.969(\frac{Gr_m D}{L_t})^{\frac{1}{2.75}} \quad \text{(for turbulent flow)} \end{aligned} \tag{17}$$

A dimensionless Grashof number based on the circulating flow rate is calculated for data analysis and compared with the steady-state corrections provided by Vijayan. Vijayan's model incorporates several assumptions, including:

- The model is one-dimensional,
- The natural circulation loop (NCL) is large-scale,
- Heat loss is negligible ($< 5\%$),
- Axial conduction and thermal viscosity effects are negligible,
- The Boussinesq approximation is applied. The Boussinesq approximation is a simplification used in the analysis of fluid flow under the influence of buoyancy forces. This approximation assumes that variations in fluid density can be ignored in the momentum term of the motion equation, except where density changes impact acceleration coefficients. By applying this approximation, solving the fluid motion equations becomes significantly easier, particularly in scenarios involving density changes.

Laminar flow in the low input power range and turbulent flow in the high input power range consistently remain in steady-state conditions (Ghorbanali and Talebi, 2020). The numerical results of this study are compared with Vijayan's steady-state corrections, the results are presented in Fig. 3.

Figure 3 provides a detailed comparison between the numerical results obtained in this study and Vijayan's corrections for steady-state flow. The graph is analyzed based on three key axes:

- Horizontal Axis: This axis represents the logarithm of $(Gr.D)/L$, where Gr is the Grashof number, D is the hydraulic diameter, and L is the characteristic length. These parameters define the flow and heat transfer conditions in the system.
- Left Vertical Axis: The left vertical axis displays the logarithm of the steady-state Reynolds number (Re_{ss}). This parameter is crucial in determining whether the flow is laminar or turbulent within the loop.
- Right Vertical Axis: The right vertical axis indicates the input power (P) in watts required to maintain the flow within the system.

The plot shown in green dashed line in Fig. 3 is Vijayan's empirical correction for laminar flow with $Re_{ss} = 0.1768(Gr.D/L)^{0.5}$, and the numerical data points obtained, shown in blue, are in perfect agreement with it.

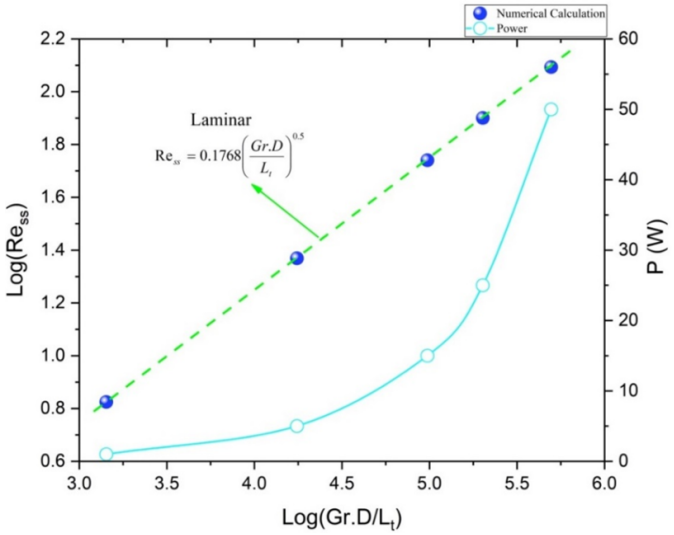

Figure 3: Closed loop natural circulation in steady state condition for mini-loop.

2.2.2 Transient state solution

By using finite difference method (FDM) for Eqs. (7) to (10), temperature distribution and mass flow rate distribution of the flow through the loop were obtained. FDM is expressed by backward formulas for spatial derivatives and forward formulas for time derivatives. After simplification, the following results can be obtained:

$$\begin{aligned} \theta_{i,n+1} =& (1 - \frac{L_t\Delta\tau}{H\Delta S}\omega_n)\theta_{i,n} + (\frac{L_t\Delta\tau}{H\Delta S}\omega_n)\theta_{i-1,n} \\ &+ \frac{L_t\Delta\tau}{L_h} \qquad \text{(heater)} \end{aligned} \tag{18}$$

$$\begin{aligned} \theta_{i,n+1} =& (1 - \frac{L_t\Delta\tau}{H\Delta S}\omega_n - St_m\Delta\tau)\theta_{i,n} \\ &+ (\frac{L_t\Delta\tau}{H\Delta S}\omega_n)\theta_{i-1,n} \qquad \text{(cooler)} \end{aligned} \tag{19}$$

$$\begin{aligned} \theta_{i,n+1} =& (1 - \frac{L_t\Delta\tau}{H\Delta S}\omega_n)\theta_{i,n} + (\frac{L_t\Delta\tau}{H\Delta S}\omega_n)\theta_{i-1,n} \\ &\text{(all sections except heater and cooler)} \end{aligned} \tag{20}$$

$$\begin{aligned} &\omega_{n+1} + \frac{pL_t\Delta\tau}{2DRe_{ss}^b}(\omega_{n+1})^{2-b} = \omega_n \\ &+ \frac{Gr_m\Delta\tau}{Re_{ss}^3}\oint\theta_{i,n+1}\mathrm{d}z \end{aligned} \tag{21}$$

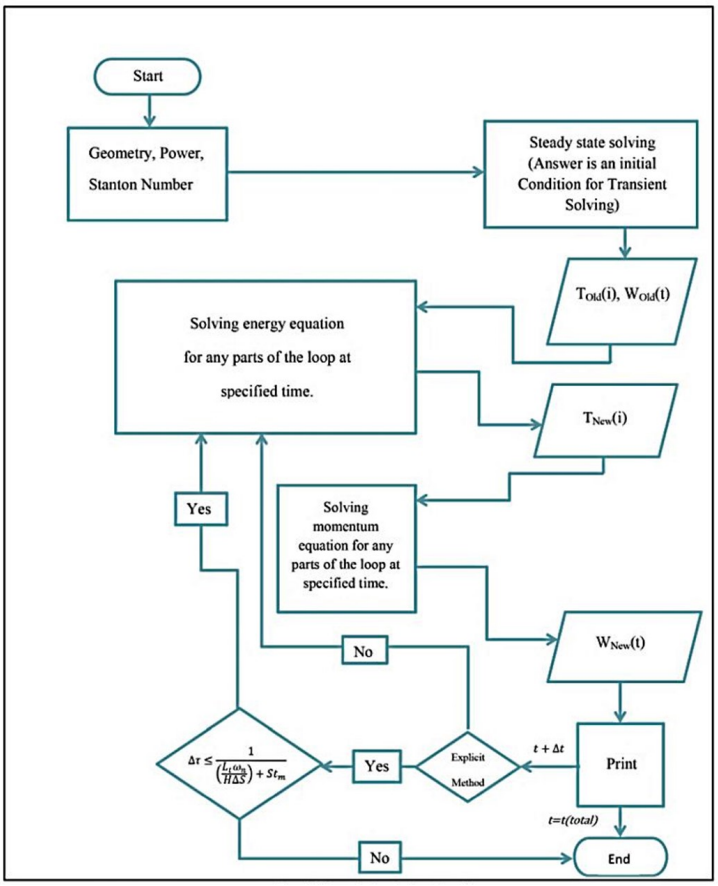

Figure 4: Numerical solution algorithm.

The numerical stability criterion for the energy equation can be expressed as:

$$\Delta\tau \leq \frac{1}{(\frac{L_t\omega_n}{H\Delta S}) + St_m} \tag{22}$$

The methodology used to solve the energy and momentum equations numerically using the finite difference method -which was created specifically for this study's computing process is shown in Fig. 4. The initial conditions for the transient solution are validated by solving the equations under steady-state conditions. The temperature is first determined from the energy equation and then applied to the momentum equation to calculate the dimensionless flow rate simultaneously. The process is iterative, with each time step using the dimensionless temperature and flow velocity values obtained from the previous step. In the explicit method, it is very important to adhere to the numerical stability criterion specified in Eq. (22). Based on these calculations, the stability map of the mini-loop has been generated and compared across different inclination angles in Fig. 5.

Figure 5 presents stability maps that illustrate the relationship between the Stanton number (St), operating power (P), and the logarithm of the Grashof number ($\log(Gr)$) across different inclination angles. The graphs reveal that within the specified power range of the mini-loop system, the stability characteristics are consistent across the various inclination angles tested, specifically at 0°, 30°, and 75°. This consistency suggests that the inclination angle does not significantly influence the stability map at these power levels. In the left graph, which plots power (P) against St, the transition from unstable to stable regions occurs at approximately similar St values regardless of the inclination angle. This indicates that the critical St for stability remains nearly the same, irrespective of the angle, reinforcing the idea that the inclination angle has a minimal effect on system stability in this context. Similarly, the right graph, which shows the relationship between $\log(Gr)$ and St, exhibits overlapping curves for all tested inclination angles. The boundary between the unstable and stable regions follows a nearly identical trend across different angles, further emphasizing that the stability behavior of the system is largely independent of the inclination angle at the power levels under consideration. In summary, the analysis of Fig. 5 supports the conclusion that the inclination angle does not play a significant role in altering the stability map of the mini-loop system within the examined power range.

2.2.3 Simulation with Ansys Fluent

The ANSYS Fluent software (ANSYS, 2024) is a well-known and efficient tool for simulating processes such as heat transfer, fluid flow, and others. Its primary use is in Computational Fluid Dynamics (CFD), which solves differential equations that cannot be solved analytically. To simulate the loop using ANSYS Fluent, several assump-

Table 1: Thermo-physical properties of loop fluid at a temperature of 25 °C and a pressure 1 atm.

Thermo-Physical Properties of Fluid	ρ (kg.m^{-3})	μ (kg.m^{-1}s^{-1})	C_p (J.kg^{-1}.°C^{-1})	β (K^{-1})	Pr
Value	997.1	0.00089	4183	0.00025	6.3

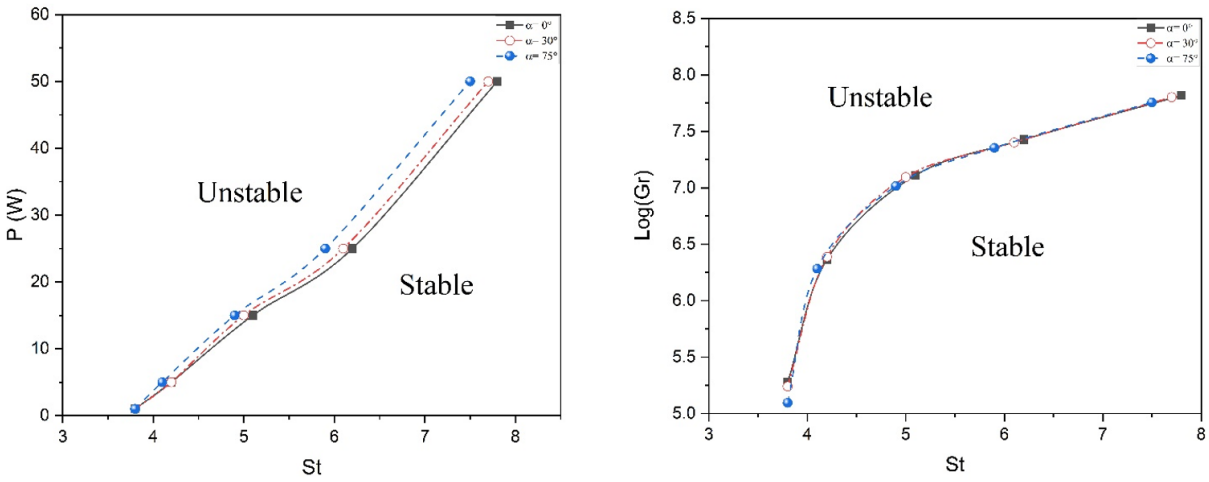

Figure 5: Stability map of mini-loop at different inclination angles.

tions were made:

1. Heat Input: Heat is introduced at the bottom of the loop (heat source) as a constant heat flux, which is varied to analyze the system's stability.

2. Cooling Mechanism: The cooling section, located at the upper part of the loop, is modeled as a heat exchanger with a constant wall temperature (Tc), representing the lowest temperature in the system. Tc is treated as a variable parameter to study its impact on stability.

3. Boussinesq Approximation: Given that the temperature variation in the problem is relatively small, the Boussinesq approximation is applied. To enhance the accuracy of the simulation, the fluid's physical properties were defined as a function of temperature using a 7th-order polynomial in the material properties section. The results obtained using detailed approach did not significantly differ from those using the Boussinesq approximation, justifying its use in the calculations.

4. Loop Geometry: It is assumed that the inner diameter of the loop is uniform throughout and is set to 5 mm.

5. Insulation Assumption: The hot and cold legs of the loop are considered insulated.

6. Neglected Effects: Axial heat transfer and thermal viscosity effects in the fluid are neglected.

The thermo-physical properties of the fluid (water) used in the simulation are detailed in Table 1, and these values were used as the initial conditions for the fluid in the simulation. Table 2 outlines several parameters relevant to the simulation of the mini-loop using ANSYS Fluent. Figure 6 shows a sample of the meshing and fluid temperature and velocity distributions in the mini-loop.

Table 2: Parameters related to simulation with Ansys Fluent software for mini-loop.

The method of solving gradients	Least squares cell based
Solving algorithm	Coupled
Spatial discretization type of pressure	Second order
Solver	Pressure Based
Flow model	$k-\omega(2eq)$
Geometry	3D Channel
Ansys fluent parameters	Mini-loop

Figure 6 illustrates the meshing and the fluid temperature and velocity distributions in the mini-loop for an operating power of 25 W. This figure not only highlights the computational mesh used for the simulations, which is essential for ensuring accuracy and stability, but also provides critical insights into the thermal performance of the system under specified conditions. The temperature and velocity distributions reveal how the fluid interacts with the mini-loop geometry, further emphasizing the effectiveness of the heat transfer process in this configuration.

3 Results and Discussion

Figure 7 illustrates the variation in the maximum temperature of the fluid over time for different operating powers (25 W, 35 W, and 45 W) in the vertical, non-inclined mini-loop system. The most important thing to notice in this case is that when a stable state of maximum fluid temperature approaches 100 °C, stable under atmospheric pressure, single-phase fluid remains in its single-phase state. For these powers the temperature initially rises above 100 °C but eventually stabilizes below this threshold. This be-

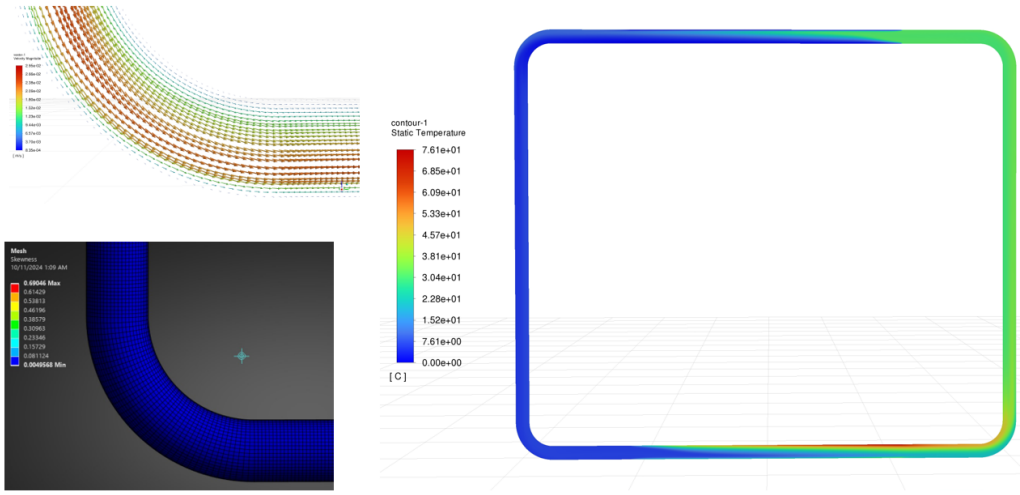

Figure 6: Meshing and fluid temperature and velocity distribution in the mini-loop at P=25W without inclination, simulated using ANSYS Fluent.

havior shows that while higher powers cause initial temperature fluctuations, the system can eventually maintain a steady state within the safe temperature range for single-phase flow. These fluctuations are observable in temperature curves because of hybrid initialization, which is used in the methodology for calculations. These results indicate that the mini-loop can be safely operated up to powers of 45 W without breaking out into two-phase flow, provided that the system is given enough time to stabilize from its initial fluctuations.

Figure 8 compares the simulation results from ANSYS Fluent with those obtained from numerical calculations for a mini-loop operating at powers of 5, 15, 25, 35, and 45 W in the vertical, non-inclined mini-loop system. The two parameters analyzed are the mass flow rate and the temperature difference across the heat source.

The comparison demonstrate that the results obtained in ANSYS Fluent are in closely align with those calculated with numerical methods, which shows the accuracy performed by Fluent simulations to reproduce the behavior of the system under study. More specifically, the mass flow rate and temperature difference graphs indicate that both variables reach a steady state, with few initial fluctuations compared to the numerical calculations using ANSYS Fluent. These initial fluctuations in the numerical calculations can be attributed to errors in the initial conditions and the numerical methods used. Notably, these initial conditions are often based on estimated or guessed values that may differ significantly from the actual parameters. On the other hand, ANSYS Fluent appears to handle these initial guesses more effectively, leading to smoother curves with fewer fluctuations and a closer approximation to the real behavior of the system. This difference highlights Fluent's robustness in dealing with transient initial conditions due to its internal advanced settings and algorithms. In both methods, the fluctuations decrease as the simulations progress, eventually reaching convergence. It should be noted that in the obtained results, it is the final stable values that are important in judging the performance of the system, not the transient fluctuations. Choosing appropriate control values in numerical calculations can reduce these initial fluctuations and cause the steady state solution to be obtained with a faster convergence speed.

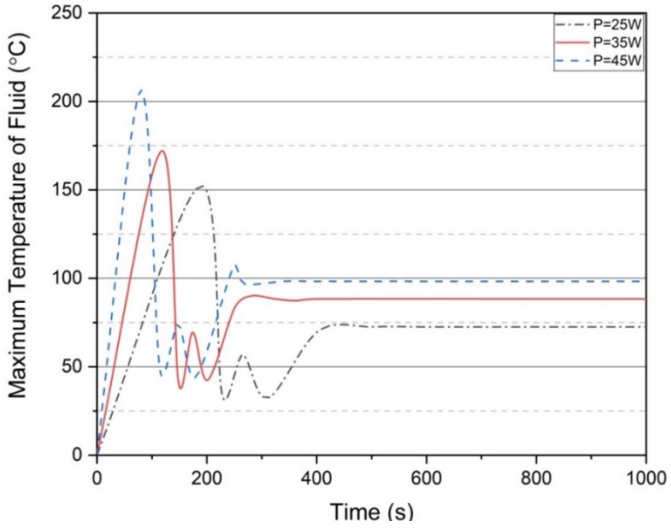

Figure 7: Maximum fluid temperature for 25, 35 and 45 W powers with Ansys Fluent.

In summary, the very good agreement of the two methods within the steady-state parts of the graphs validates the reliability of ANSYS Fluent for simulating the mini-loop's behavior at different power levels. To examine the effect of inclination angle on the thermo-hydraulic parameters of the mini-loop, simulations were performed using ANSYS Fluent at inclination angles of 0°, 30°, and 75°. For better comparison, three different power levels of 2.5, 7.5 and 10 W were selected for analysis. The resulting data, which provide insight into how the inclination angle influences the mini-loop's performance at these varying power levels, are presented in Fig. 9.

The graphs presented in Fig. 9 depict the influence of inclination angle on the natural circulation parameters of a mini-loop. It can be seen that for a constant power, the value of mass flow rate changes according to the in-

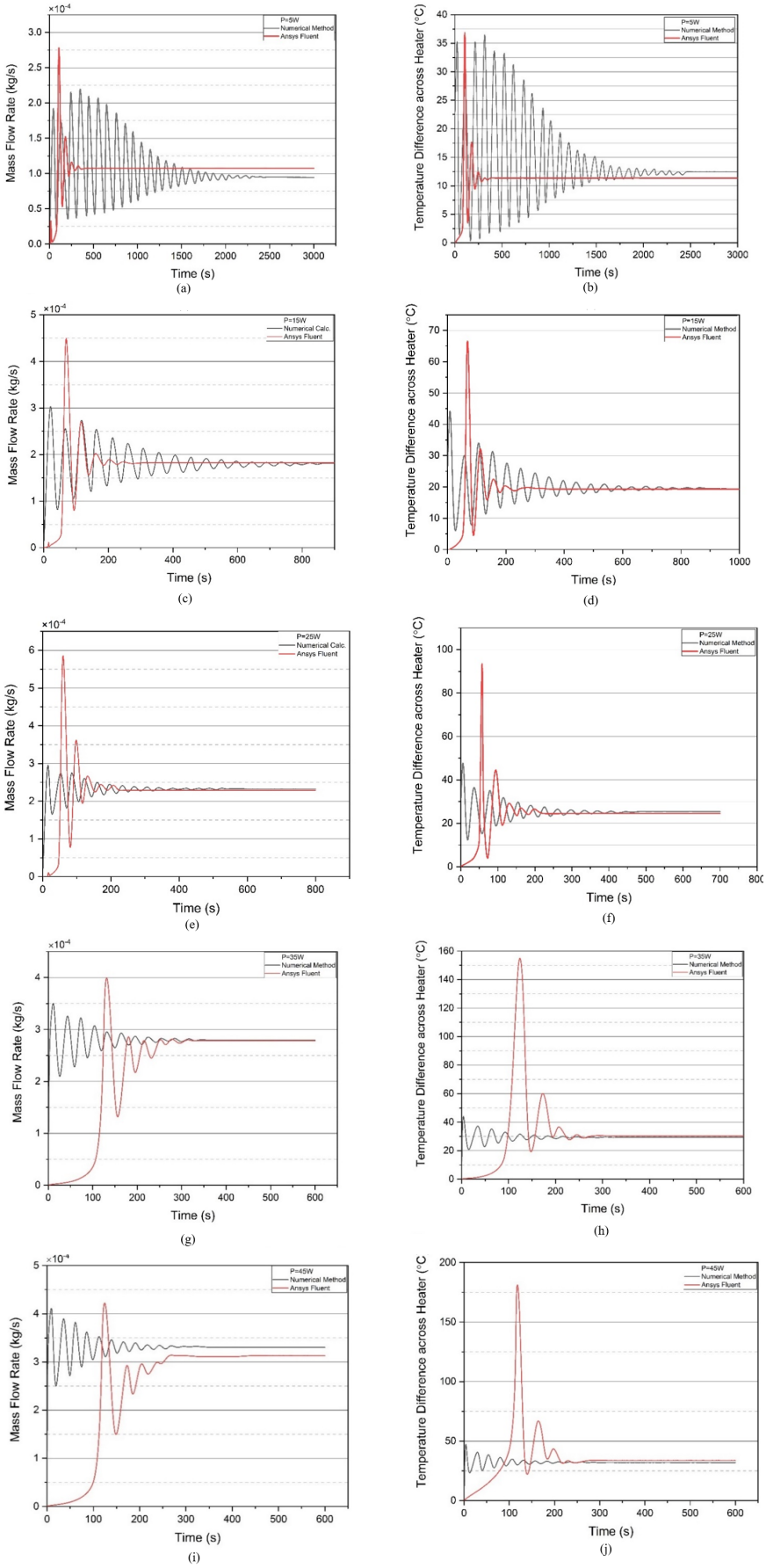

Figure 8: Comparison of Ansys Fluent simulation and numerical solution results for powers of 5, 15, 25, 35 and 45 W.

clination angle. Mass flow rate has the maximum value when there is zero inclination (i.e., without any tilt) and

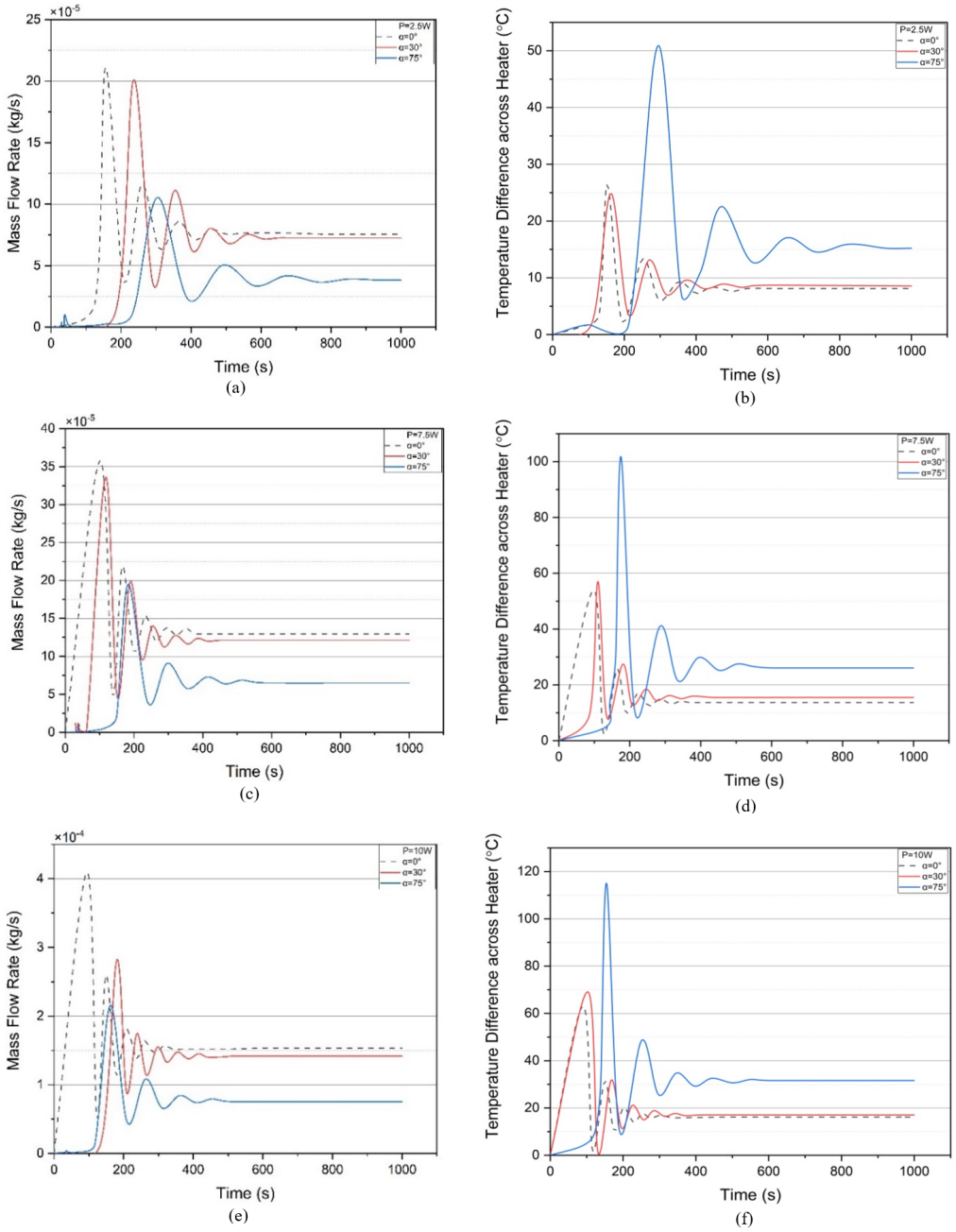

Figure 9: The influence of inclination angle on the natural circulation parameters of mini-loop using Ansys Fluent software.

its value decreases with increasing values of the inclination angle. Additionally, the angle of inclination also has an effect on the temperature difference across the heat source. It can be seen that with the gradual increase in the angle of inclination, for a given power, the temperature difference between the two ends of the heat source increases. The temperature difference increases, as expected, with a decrease in mass flow rate. These graphs further show that with adjustment in the angle of inclination, it is possible to have a required temperature difference with lower power. For example, if one compares the temperature difference across the heat source at zero degrees of inclination with 25 W to that with 75 degrees of inclination and a power of 7.5 W, one would see this correspondence (as shown in Fig. 8-f and Fig. 9-d). This indicates that by modifying the loop's inclination angle, one can control the mass flow rate and increase the output temperature at a lower power. Overall, these findings suggest that adjusting the inclination angle can effectively control the mini-loop's performance, allowing for precise adjustments in both temperature and mass flow rate.

4 Conclusions

The numerical simulations and CFD analysis conducted in this study provide a comprehensive understanding of the effects of inclination angle on the natural circulation performance of a mini-loop. The numerical results were compared with Vijayan's steady-state corrections, as depicted in Fig. 3. The data points show excellent agreement with

Vijayan's empirical correction for laminar flow conditions, confirming that the flow within the mini-loop remains in the laminar regime under the examined conditions. This alignment validates the accuracy of the numerical model in predicting the flow behavior in natural circulation loops, demonstrating that the simplified assumptions used in the model are appropriate for such applications.

The stability maps presented in Fig. 5 illustrate the relationship between the Stanton number (St), operating power (P), and the logarithm of the Grashof number (Log (Gr)) across different inclination angles. The analysis reveals that within the operational power range of the mini-loop (up to 50 W), the stability characteristics remain consistent across the various inclination angles tested (0°, 30°, and 75°). This consistency suggests that the inclination angle does not significantly affect the stability map at these power levels. The transitions between stable and unstable regions occur at similar Stanton numbers, regardless of the inclination angle, reinforcing the conclusion that inclination angle has a minimal effect on the stability of the system within the studied range.

The study demonstrates that increasing the inclination angle of the loop leads to a decrease in the mass flow rate and an increase in the temperature difference across the heat source. This trend is consistent across different power levels and inclination angles, as shown in Figs. 8 and 9. Specifically, for an inclination angle of 0 degrees with a power of 25 W and an inclination angle of 75 degrees with a power of 7.5 W, a temperature difference of approximately 26 degrees Celsius was observed (Figs. 8-f and 9-d). This finding suggests a practical approach for optimizing the thermal performance of natural circulation systems by modifying the geometric configuration rather than the operational conditions.

The results obtained from CFD simulations using ANSYS Fluent closely match those from the numerical calculations, both showing good agreement with the experimental data and theoretical models. This consistency across different methodologies confirms the reliability of the numerical and CFD approaches in modeling natural circulation behavior, supporting their use for further studies on more complex systems.

The findings suggest that the inclination angle is a key parameter in controlling the performance of natural circulation systems. By optimizing the inclination angle, it is possible to achieve desired thermal conditions without changing power levels, which can be particularly beneficial in applications such as passive cooling systems in nuclear reactors. This approach allows for flexible and efficient design adjustments, enhancing system stability and performance under varying operational conditions.

Overall, this study provides valuable insights into the thermal-hydraulic behavior of natural circulation mini-loops and highlights the importance of inclination angle in system optimization. Valid numerical models provide a strong foundation for future research and development, focusing on the optimization of natural circulation systems in a wide range of industrial applications. Further studies are needed to investigate more realistic and varied conditions, including a wider range of fluid properties -such as nanofluids- and more geometries for the loop in order to increase the applicability and reliability of these findings.

Conflict of Interest

The authors declare no potential conflict of interest regarding the publication of this work.

References

Adarsh, R., Raveesh, G., and Rupesh, S. (2020). Orifice enabled flow stabilization of natural circulation loop at lower inclinations. *Kerntechnik*, 85(3):140–146.

Ahmed, N. M., Gao, P., and Bello, S. (2020). Natural circulation systems in nuclear reactors: advantages and challenges. In *IOP Conference Series: Earth and Environmental Science*, volume 467, page 012077. IOP Publishing.

ANSYS (2024). ANSYS fluent tutorial guide. Canonsburg, PA.

Bejjam, R. B. and Kiran Kumar, K. (2019). Numerical investigation to study the effect of loop inclination angle on thermal performance of nanofluid-based single-phase natural circulation loop. *International Journal of Ambient Energy*, 40(8):885–893.

Bocanegra, J. A., Marchitto, A., and Misale, M. (2022). Thermal performance investigation of a mini natural circulation loop for solar PV panel or electronic cooling simulated by lattice boltzmann method. *Int. J. EQ*, 5:1–12.

Borreani, W., Chersola, D., Lomonaco, G., et al. (2017). Assessment of a 2D CFD model for a single phase natural circulation loop. *Int. J. Heat Technol.*, 35(Special Issue 1):S300–S306.

Chen, K. (1985). On the oscillatory instability of closed-loop thermosyphons.

Chen, Y. and Yang, Z. (2022). Probability Safety Analysis for Nuclear Power Plant Long-Term Temporary Shutdown State. In *International Conference on Nuclear Engineering*, volume 86489, page V013T13A021. American Society of Mechanical Engineers.

Garibaldi, P. and Misale, M. (2008). Experiments in single-phase natural circulation miniloops with different working fluids and geometries.

Ghorbanali, Z. and Talebi, S. (2020). Investigation of a nanofluid-based natural circulation loop. *Progress in Nuclear Energy*, 129:103494.

IAEA (2021). *Natural circulation in advanced water-cooled reactors: Recent developments and future directions (IAEA-TECDOC-1861)*. International Atomic Energy Agency (IAEA).

Karami, I. and Aghaie, M. (2017). Sensitivity analysis of numerical schemes in natural cooling flows for low power research reactors. *Advances in Energy Research*, 5(3):255.

Kim, K. M., Jeong, Y. S., Kim, I. G., et al. (2016). Development of passive in-core cooling system for nuclear safety using hybrid heat pipe. *Nuclear Technology*, 196(3):598–613.

Luo, Q., Zhou, Y., Huang, J., et al. (2024). A review of supercritical fluid flow instability. *Progress in Nuclear Energy*, 176:105376.

Marchitto, A. and Misale, M. (2018). Mathematical modelling of engineering problems. *Journal homepage: http://iieta.org/Journals/MMEP*, 5(3):161–167.

Misale, M. (2014). Overview on single-phase natural circulation loops. In *Proc. of the intl. Conf. on advances in mechanical and automation engineering–MAE*, volume 2014.

Misale, M., Garibaldi, P., Passos, J., and De Bitencourt, G. G. (2007). Experiments in a single-phase natural circulation mini-loop. *Experimental Thermal and Fluid Science*, 31(8):1111–1120.

Moussavian, S. K., Misale, M., DAuria, F., et al. (2003). Stability behavior of single-phase natural circulation loop. In *ASME International Mechanical Engineering Congress and Exposition*, volume 37157, pages 119–131.

Nourashrafeddin, S. A., Shayesteh, M., and Bahonar, M. (2023a). Investigating the influence of inclination angle on thermohydraulic parameters of natural circulation laboratory mini-loop. *Iranian Nuclear Conference*.

Nourashrafeddin, S. A., Shayesteh, M., and Bahonar, M. (2023b). Simulation and investigation of the thermohydraulic parameters of the natural circulation loop of the university of genoa. *Iranian Nuclear Conference*.

Vijayan, P., Nayak, A., Saha, D., et al. (2008). Effect of Loop Diameter on the Steady State and Stability Behaviour of Single-Phase and Two-Phase Natural Circulation Loops. *Science and Technology of Nuclear Installations*, 2008(1):672704.

Vijayan, P., Sharma, M., and Saha, D. (2007). Steady state and stability characteristics of single-phase natural circulation in a rectangular loop with different heater and cooler orientations. *Experimental Thermal and Fluid Science*, 31(8):925–945.

Zhu, H., Yang, X., Lian, H., et al. (2013). Experimental and Numerical Study on Natural Circulation Under Inclined Condition. In *International Conference on Nuclear Engineering*, volume 55799, page V002T03A021. American Society of Mechanical Engineers.

Zweibaum, N. (2015). *Experimental validation of passive safety system models: Application to design and optimization of fluoride-salt-cooled, high-temperature reactors*. University of California, Berkeley.

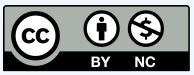

To cite this article:

Nourashrafeddin, S. A. and Shayesteh, M. (2025). Numerical and CFD analysis of inclination angle effects on natural circulation mini-loop performance. Radiation Physics and Engineering, 6(2), 23-34. doi: 10.22034/rpe.2024.476581.1240

DOI: 10.22034/rpe.2024.476581.1240

To link to this article: https://doi.org/10.22034/rpe.2024.476581.1240